

Investigation of NIR Spectroscopy and Electrical Resistance-Based Approaches for Moisture Determination of Logging Residues and Sweet Sorghum

Sung-Wook Hwang,^a Hyunwoo Chung,^b Taekyeong Lee,^a Hyo Won Kwak,^{a,b,c}
In-Gyu Choi,^{a,b,c} and Hwanmyeong Yeo^{a,b,c,*}

Techniques based on electrical resistance and near-infrared (NIR) spectroscopy were used to determine the moisture content (MC) of logging residues and sweet sorghum. The MC of biomass is a factor to be controlled that can affect the quality of final products. To accurately measure the moisture in fragmented materials, it is essential to increase the bulk density of the materials by compression. The low bulk density increased the error from the oven-drying MC and the variation between repeated measurements. The calculated correction factor made it possible to use a commercial wood moisture meter for biomass materials. Ordinary least squares regression models built with the electrical resistance data achieved coefficients of determination (R^2) of 0.933 and 0.833 with root mean square errors (RMSE) of 0.505 and 0.891, respectively, for the MC predictions of logging residue and sweet sorghum. Partial least squares regression models combined with NIR spectroscopy achieved R^2 of 0.942 and 0.958 with RMSE of 1.318 and 3.681 for logging residue and sweet sorghum, respectively. In contrast to the electrical resistance-based models, the NIR-based models could predict the MC regardless of the bulk density of the materials. Data transformation by the second derivative and removal of outliers contributed to the improvement of the prediction of the NIR-based models.

DOI: 10.15376/biores.18.1.2064-2082

Keywords: Biomass; Electrical resistance; Moisture content; Moisture meter; Near-infrared spectroscopy; Outlier detection; Partial least squares

Contact information: a: Research Institute of Agriculture and Life Sciences, Seoul National University, 1 Gwanak-ro, Gwanak-gu, Seoul 08826, Republic of Korea; b: Department of Forest Sciences, College of Agriculture and Life Sciences, Seoul National University, 1 Gwanak-ro, Gwanak-gu, Seoul 08826, Republic of Korea; c: Department of Agriculture, Forestry and Bioresources, College of Agriculture and Life Sciences, Seoul National University, 1 Gwanak-ro, Gwanak-gu, Seoul 08826, Republic of Korea;

* Corresponding author: hyeo@snu.ac.kr

INTRODUCTION

Lignocellulosic biomass is the most abundant natural renewable resource and has recently attracted attention as a substitute for petroleum resources owing to global warming and environmental pollution (Qian 2014). Accordingly, the market for biorefinery materials continues to increase with the transition from the petroleum to the biochemical industry (Costa and De Morais 2011; Erickson *et al.* 2012). In pursuing economical biorefining using lignocellulosic biomass, unused forest biomass left on site from logging offers great potential (Swinton *et al.* 2021). Logging residues, which mainly consist of

branches, twigs, and top parts of trees, account for approximately 36% of untapped potential feedstock (Langholtz *et al.* 2016). As a comprehensive strategy for ‘Net zero by 2050’ (Bouckaert *et al.* 2021), the Korean government aims to promote the use of wood and forest biomass and is planning to increase the annual log production and collection rate of unused forest biomass (United Nations 2020). In this context, logging residues have great potential to become a stable biomass source in Korea in the future.

While many studies have reported the development of high-value-added and high-functional materials using biomass feedstocks (Takagaki *et al.* 2012; Kalyani and Anitha 2013; Molino *et al.* 2016; Park *et al.* 2019; Hwang *et al.* 2021c; Cywar *et al.* 2022), studies on the precise moisture evaluation of biomass materials during storage have been relatively few (Samuelsson *et al.* 2006; Julrat and Trabelsi 2019). Fresh biomass contains large amounts of water (Ekefre *et al.* 2017; Eliasson *et al.* 2020), and the moisture content (MC) varies with plant species type and season (McKendry 2002; Filbakk *et al.* 2011). Moisture in biomass feedstocks causes high transportation costs, so they are often left at harvest sites or along roadsides to induce natural drying (Filbakk *et al.* 2011). High MC and ambient humidity during the storage of biomass feedstock can lead to microbial infections, such as fungi and bacteria (Suchomel *et al.* 2014; Krzyżaniak *et al.* 2016; Ashman *et al.* 2018; Gejdoš and Lieskovský 2021). As biomass deterioration can cause self-heating, decay, weight loss, and failure of the biorefinery process, moisture management of biomass materials by accurate MC evaluation is essential. The MC of biomass feedstock also affects the quality and yield of the final products.

Electrical resistance is the most common approach for moisture measurement in wood (Brischke *et al.* 2008; Björngrim *et al.* 2016; Hwang *et al.* 2021a). Although the reliable range of moisture determination is limited, most portable commercial moisture meters for biomass are based on electrical resistance. Electrical methods must include control of wood species, internal stress, preservatives, and distance between electrodes for precise moisture determination of solid wood (Lahtela *et al.* 2014; Dietsch *et al.* 2015; Hwang *et al.* 2023). However, to measure biomass moisture, the compression of the fine material to create the charge travel path must be considered first (Govett *et al.* 2010).

NIRS has been favored for predicting the physical and chemical properties of lignocellulosic materials, as it enables rapid and non-destructive analysis (Mitsui *et al.* 2008; Eom *et al.* 2010; Inagaki *et al.* 2010; Via *et al.* 2014; Yang *et al.* 2015; Hwang *et al.* 2016; Horikawa 2017; Hwang *et al.* 2021b). Because NIRS acquires data through contact between a material and a probe, it may have lower or even no material compression requirements than electrical methods. However, multiple measurements are recommended because this method measures a tiny spot. In addition, due to the nature of the production and collection of biomass feedstock, some foreign substances mixed in the material may create outliers. Because outliers deteriorate moisture prediction performance, research on controlling them is required. The high cost of building a NIRS system can be a barrier to its application.

As part of a bioplastics development project, this study aims to develop techniques for rapid and precise determination of moisture in logging residues and sweet sorghum straws. Because both materials are representative lignocellulosic and herbaceous biomass available in large quantities in Korea, the project selected them as feedstock. The MC of materials is a factor that may affect the production of biomass-based monomers and plasticizers. This study investigated electrical and spectroscopic methods for moisture determination in biomass. The correction factors for measuring the biomass MC of an

electrical resistance-based commercial wood moisture meter were calculated, and MC prediction models were developed using the electrical resistance and near-infrared (NIR) spectral data acquired from the biomass feedstocks. Additionally, a technique for removing NIR spectral outliers caused by foreign substances mixed in the material was investigated. The technologies for precise moisture determination of biomass could contribute to preventing feedstock deterioration and maintaining consistent quality in the final product.

EXPERIMENTAL

Samples and Humidification

Logging residues and sweet sorghum (*Sorghum bicolor* var. *dulciusculum*) straw were used as the biomass material for moisture determination (Fig. 1). Specimens of 10 g of each of the materials were used in all experiments. Logging residues comprised comminuted amorphous woody fragments, also called hog fuel, and residues left at the site after timber harvesting operations. The bulk densities of both materials were lower than those of reported values (Jensen *et al.* 2006; Cardoso *et al.* 2013; Tang *et al.* 2014) due to their long particle size and origin, resulting in low biomass characteristics index (BCI) (Table 1).



Fig. 1. Shapes of logging residue (a) and sweet sorghum samples (b) for moisture measurement

Table 1. Details of Biomass Samples Tested

Biomass	Particle Size (mm)	Bulk Density (g/cm ³)	Reference Bulk Density (g/cm ³)	MC (%)	BCI
Logging residue	4.8 to 103.9	0.125	0.18 to 0.21 ¹⁾	11.6	11,050
Sweet sorghum	22.2 to 131.7	0.103	0.24 ²⁾	11.0	9,167

Notes: MC, moisture content; BCI, biomass characteristics index; ¹⁾ Jensen *et al.* 2006; ²⁾ Cardoso *et al.* 2013

For moisture level adjustment, the samples were conditioned stepwise in a climate chamber (HB-105MP. Hanbaek Scientific Co., Bucheon-si, Korea) at predefined temperatures and relative humidity (RH) values, as listed in Table 2. The climatic conditions tested corresponded to the equilibrium moisture content (EMC) range of 5.2 to 24.3%. After all humidification cycles were completed, the MC of the samples was determined using the oven drying method. The oven drying method was used as the reference method for MC determination (Bergman 2010).

Table 2. Environmental Conditions and Corresponding Equilibrium Moisture Contents of Biomass

RH (%)	Equilibrium Moisture Content (%)		
	Temperature (°C)		
	10	20	30
25	5.5	5.4	5.2
40	7.9	7.7	7.5
60	11.2	11.0	10.6
80	16.4	16.0	15.5
95	24.3	23.9	23.4

Sample Compression for Data Acquisition

The charge transport path may be incomplete in the logging residue and sweet sorghum samples because the narrow and elongated fragments were sparsely aggregated. This structure causes unstable electrical resistance. Hence, in this study, the moisture in the biomass was measured for materials compressed by a cylinder. A plunger compressed 10 g of samples using a high-density polyethylene plate in a cylinder 45 mm in diameter. Moisture data were obtained using a wood moisture meter, megohmmeter, and NIR spectrometer when the bulk densities of the samples were 0.09, 0.11, 0.13, 0.16, 0.21, and 0.32 g/cm³. For logging residue, because the bulk density of the raw material was 0.125 g/cm³ (Table 1), it was compressed in the range of 0.13 to 0.32 g/cm³. In stepwise compression of both materials, the bulk density of the first stage is the uncompressed state. The data were acquired by drilling holes in the end section of the compression cylinder, after which electrodes and an NIR probe were inserted. All measurements were performed in a climate chamber to minimize moisture changes in the samples. As shown in Fig. 2, a commercial wood moisture meter, electrical resistance, and NIRS were employed for moisture measurement of the biomass materials. Moisture data of the samples were obtained from compressed materials using all the moisture determination methods when the samples reached a constant weight under each climatic condition.

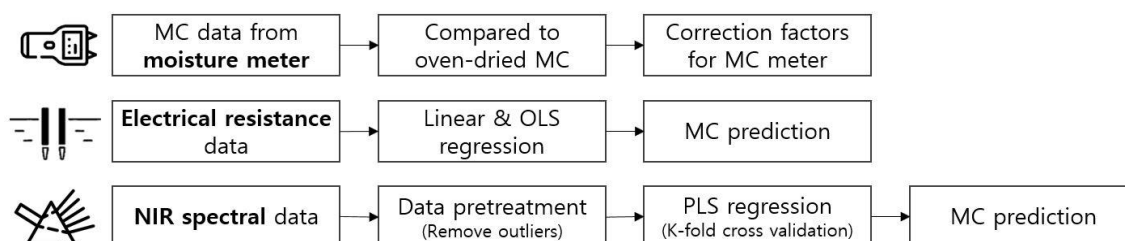


Fig. 2. Pipelines of approaches for moisture measurement in biomass materials. Notes: MC, moisture content; NIR, near-infrared; OLS, ordinary least squares; PLS, partial least squares

Moisture Meter

An electrical resistance-based wood moisture meter (MC-460; Exotek Instruments, Fichtenberg, Germany) with a general-purpose 2-pin probe was used for MC measurement. The moisture meter was designed for moisture measurement in wood, boards, chips, cardboards, and pellets in the MC range of 3 to 140%; manual temperature compensation was also possible. Correction factors for the MC of logging residue and sweet sorghum determined by the moisture meter were calculated from the comparison between the MCs measured by the moisture meter and those measured by the oven-drying method.

Electrical Resistance Measures

The electrical resistance of the biomass materials was measured using two electrodes insulated with polytetrafluoroethylene except at the tip. The distance between the electrodes was 25 mm. To maintain this distance, electrodes were fixed to a probe (26-ES, Delmhorst Instrument Co., Towaco, NJ). Electrode penetration depth was adjusted for each bulk density to measure the MC at the center of the in-cylinder compressed samples.

A super megohmmeter (SM-8220, HIOKI E. E. Corp., Nagano, Japan) was used to measure the electrical resistance of the samples. The megohmmeter passed a constant direct current voltage into the sample, measured the current at that time, and calculated the electrical resistance from the relationship between the voltage, current, and resistance. Regression equations for MC prediction were calculated for each temperature condition tested using simple linear regression on electrical resistance and oven-drying-based MC measurements. Additionally, ordinary least squares regression (OLSR) models using the relationship among MC, temperature, and electrical resistance were built for MC prediction. The OLSR models were built using Python 3.8 with open-source libraries.

Multivariate Analysis with NIR Data

Spectral dataset

NIR spectra were acquired from the biomass samples using an NIR spectrometer (NIR Quest, Ocean Insight, Orlando, FL, USA) equipped with a fiber optic probe with a scan diameter of 5 mm in reflection mode. The spectrum had a wavelength of 870 to 2500 nm with a spectral resolution of 6.6 nm and was the average of 16 scans. Because NIR characterizes shallow spots on the material surface, the spectra were measured three times at different points for each bulk density of the compressed material. Consequently, 180 spectra for the logging residue dataset and 270 spectra for the sweet sorghum dataset were collected for all climatic conditions, resulting in a database consisting of 450 NIR spectra.

From the full wavelength range of 870 to 2500 nm, noisy and non-informative regions were eliminated so that all spectra had a wavelength ranging from 1250 to 2300 nm. Subsequently, the original spectra were transformed into second derivative spectra using a Savitzky–Golay filter (Savitzky and Golay 1964) with 11 points and a quintic polynomial. Such spectral selection and transformation may improve model performance by increasing data precision (Hwang *et al.* 2016; 2021b).

Clustering

Principal component analysis (PCA) was performed to analyze the spectral changes in logging residues and sweet sorghum induced by moisture and bulk density variations. PCA transformed the 1250 to 2300-nm NIR spectra, as a 165-dimensional spectral vector, into 6 principal components (6-dimensional vector). Variations in data due to moisture changes were analyzed using principal component (PC) score plots and loadings.

Density-based spatial clustering of applications with noise (DBSCAN) (Ester *et al.* 1996; Zhang *et al.* 2004) was employed to detect outliers from the data points projected onto the PC orthogonal coordinate system. The DBSCAN clustering parameters epsilon (*esp*) and the minimum number of samples (*min_samples*) were empirically selected as 0.1 and 3, respectively. The parameter '*esp*' is the distance of influence of data points to determine valid neighbors, and '*min_samples*' is the minimum number of data points required to create a cluster. Three or more consecutive points within a distance of 0.1 from a data point are considered a cluster.

Moisture prediction model

Partial least squares regression (PLSR) models (Abdi 2010) were built to predict the MC of the biomass materials. The models used the 165-dimensional NIR spectra as the input variables and MC as the output variable. The model was verified using k-fold cross validation (Fig. 3). Data folds were created for each bulk density, resulting in four-fold data for logging residue and six-fold data for sweet sorghum. In other words, the datasets were divided into calibration and prediction sets at a ratio of 1:3 for logging residue and 1:5 for sweet sorghum. This data partitioning was intended to independently generate calibration and prediction sets by bulk density. The coefficient of determination (R^2) and root-mean-square error (RMSE) were used as performance metrics for the PLSR models.

$$R^2 = 1 - \left(\sum_i (M_i - \hat{M}_i)^2 / \sum_i (M_i - \mu)^2 \right) \tag{1}$$

$$RMSE = \sqrt{\frac{1}{n} \sum_{i=1}^n (\hat{M}_i - M_i)^2} \tag{2}$$

where M_i and \hat{M}_i are the measured and predicted MCs of the i^{th} observation, respectively. The parameter μ is the overall mean and n is the total number of observations. All processes were performed using Python 3.8, including data preprocessing, clustering, and prediction model construction.

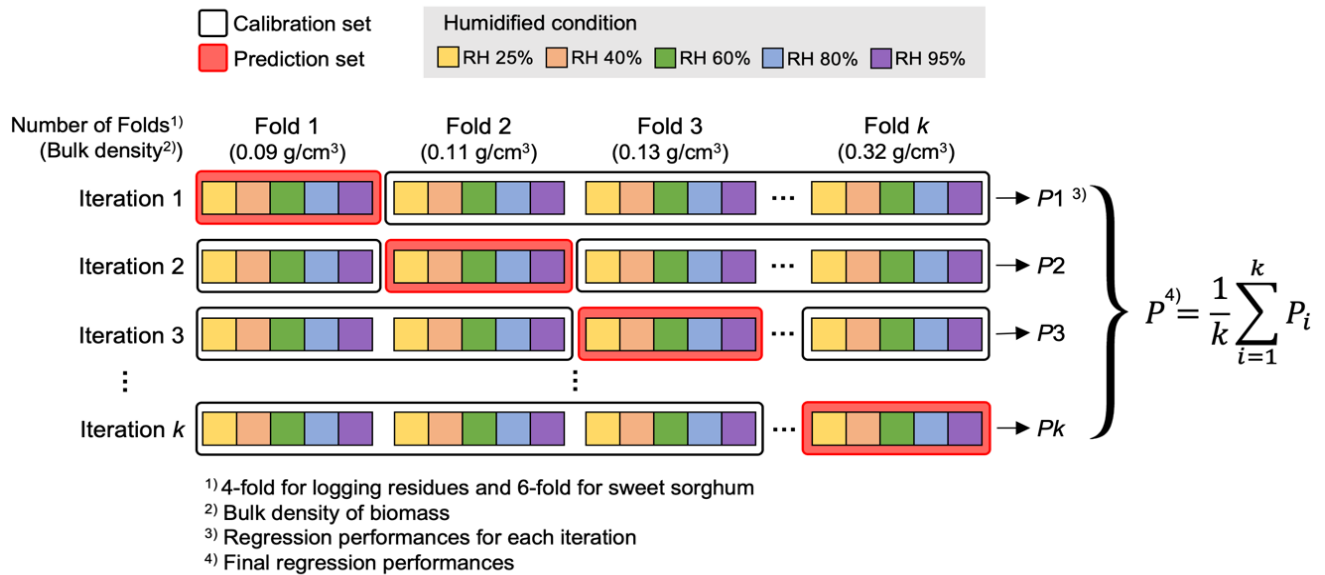


Fig. 3. Schematic diagram of k-fold cross-validation to build models for measuring moisture content of biomass materials

RESULTS AND DISCUSSION

Moisture Meter

Moisture meters are sensitive to material or product characteristics and environmental conditions. Generally, commercial moisture meters establish standard models for selected species and apply correction factors for other species (Gillis *et al.* 2001). The correction factors manufacturers provide are inevitably limited, even more so in different countries and climate zones. Suppose that the wood species or material to be measured is not listed in the moisture meter. In that case, the user often selects the one most similar to the target species, which inevitably entails errors. The calculation of the correction factor is to improve the accuracy of the moisture meter for a specific target.

Figure 4 presents the MCs of the biomass measured using a moisture meter and oven-drying.

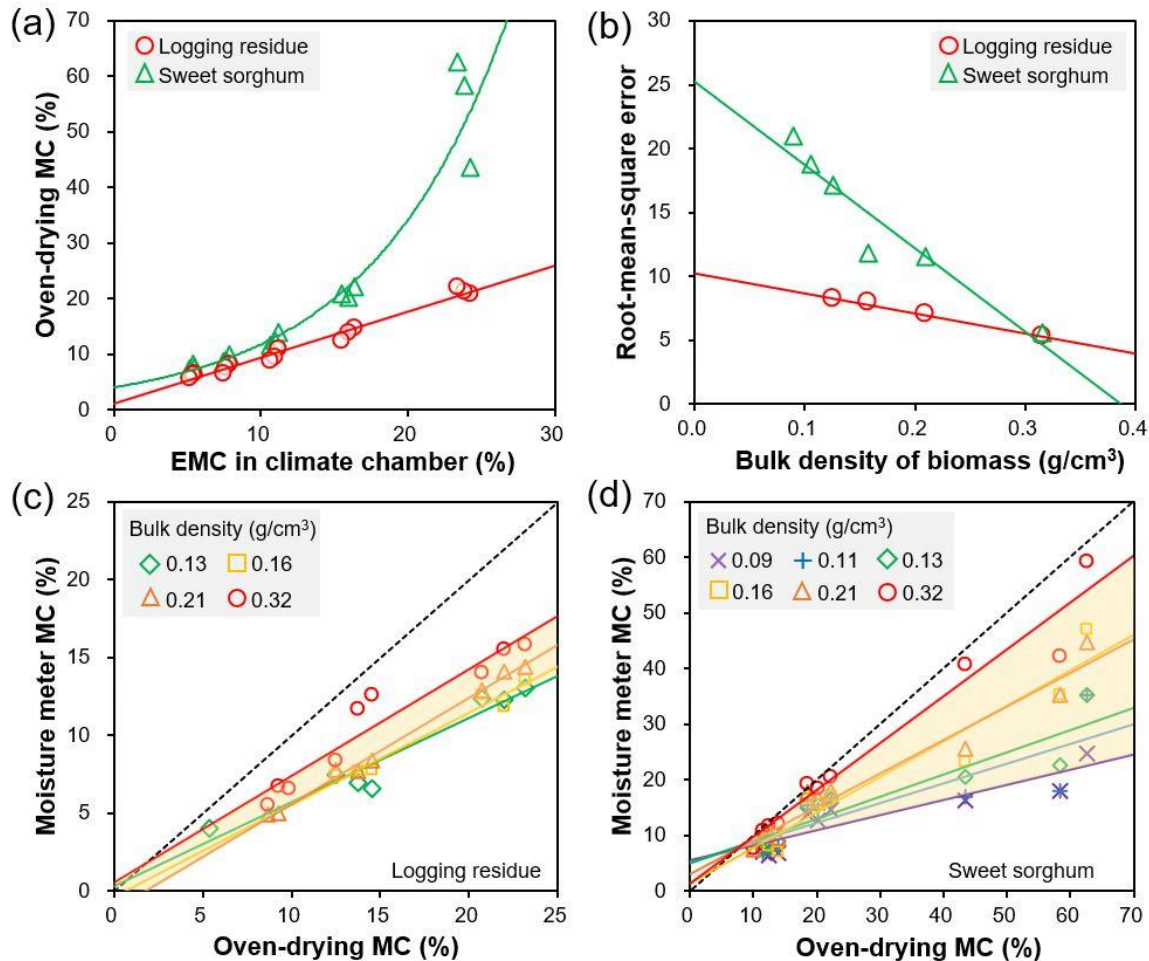


Fig. 4. Relation of moisture content (MC) measured by oven-drying method and moisture meter. MC of biomass measured by oven-drying method (a), root mean square errors of moisture meter MC for oven-drying MC (b), and relation of oven-drying MC and moisture meter MC for logging residue (c) and sweet sorghum (d)

The relationship between the biomass MCs measured using the oven-drying method and the EMCs in the climate chamber differed depending on the material (Fig. 4a). The logging residue MCs were slightly lower than that of the in-chamber EMCs and showed a linear relationship. Contrastingly, the MC of sweet sorghum was higher than the EMC of the chamber and had an exponential regression line due to sweet sorghum absorbing excessive moisture above the fiber saturation point (FSP) during humidification at 95% RH. The high MC of sweet sorghum is attributed to its high proportion of hydrophilic components. Compared with wood, sweet sorghum has a low content of lignin (hydrophobic component) and a high hemicellulose content (hydrophilic component) (Fajardo *et al.* 2015).

Increasing the bulk density of the materials decreased the RMSEs between the MCs and oven-drying MCs (Fig. 4b), which suggests that creating a material with a high bulk density is advantageous for reliable moisture determination. The importance of material compression can also be seen in that the MCs approach oven-drying MCs at higher bulk densities (Figs. 4c and 4d). The correction factors and RMSEs of the moisture meter MC at a bulk density of 0.32 g/cm³ for the oven-drying MCs are listed in Table 3. The RMSEs of the correction factors, 1.46 MC – 0.51 for logging residue and 1.19 MC – 1.42 for sweet sorghum, were reduced from 4.64 to 1.58 and from 5.33 to 3.96, respectively. The tested moisture meter achieved a relatively low RMSE for logging residues, probably because the device was originally designed for woody materials. By applying a correction factor to the MC measured by the moisture meter, the trend line of the corrected MC for both materials moved very close to the line of the reference MC by oven drying (Fig. 5). The correction factor enabled the use of a moisture meter for herbaceous biomass, *i.e.*, sweet sorghum.

Table 3. Correction Factors for Moisture Contents Measured by Moisture Meter Tested

Biomass	Correction Factor	RMSE	
		Original MC	Corrected MC
Logging residue	1.46 MC – 0.51	4.64	1.58
Sweet sorghum	1.19 MC – 1.42	5.33	3.96

Notes: RMSE, root mean square error; MC, moisture content measured by a moisture meter

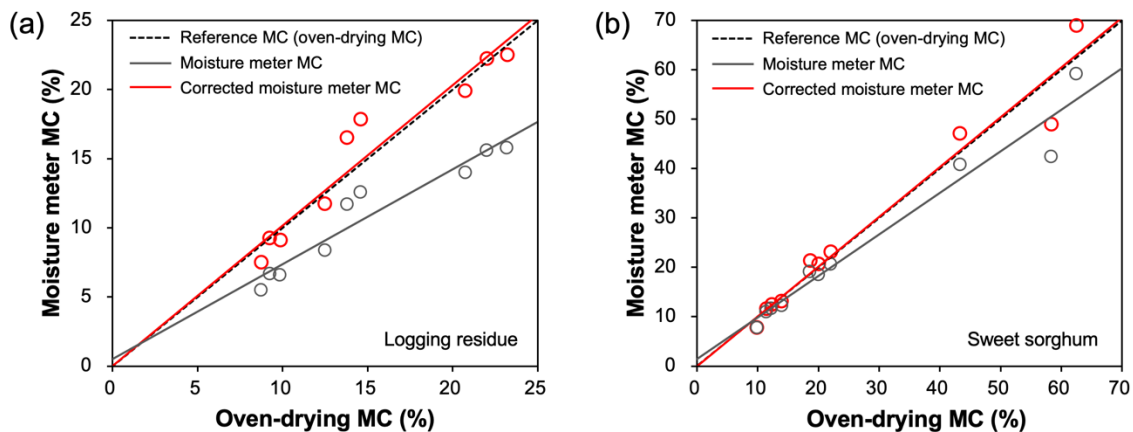


Fig. 5. Relation of oven-drying moisture content (MC), moisture meter MC, and moisture meter MC with correction factor applied: (a) Logging residue; (b) Sweet sorghum. Moisture meter MCs are measured at a bulk density at 0.32 g/cm³.

Electrical Resistance

Figure 6 shows the electrical resistance of logging residues and sweet sorghum straw measured using the 2-pin method. An increase in MC resulted in a decrease in electrical resistance, and an increase in bulk density at a specific MC also caused a decrease in electrical resistance (Figs. 6a and 6b). As with the MC measurements, the increase in bulk density contributed to the creation of continuous paths for charge travel.

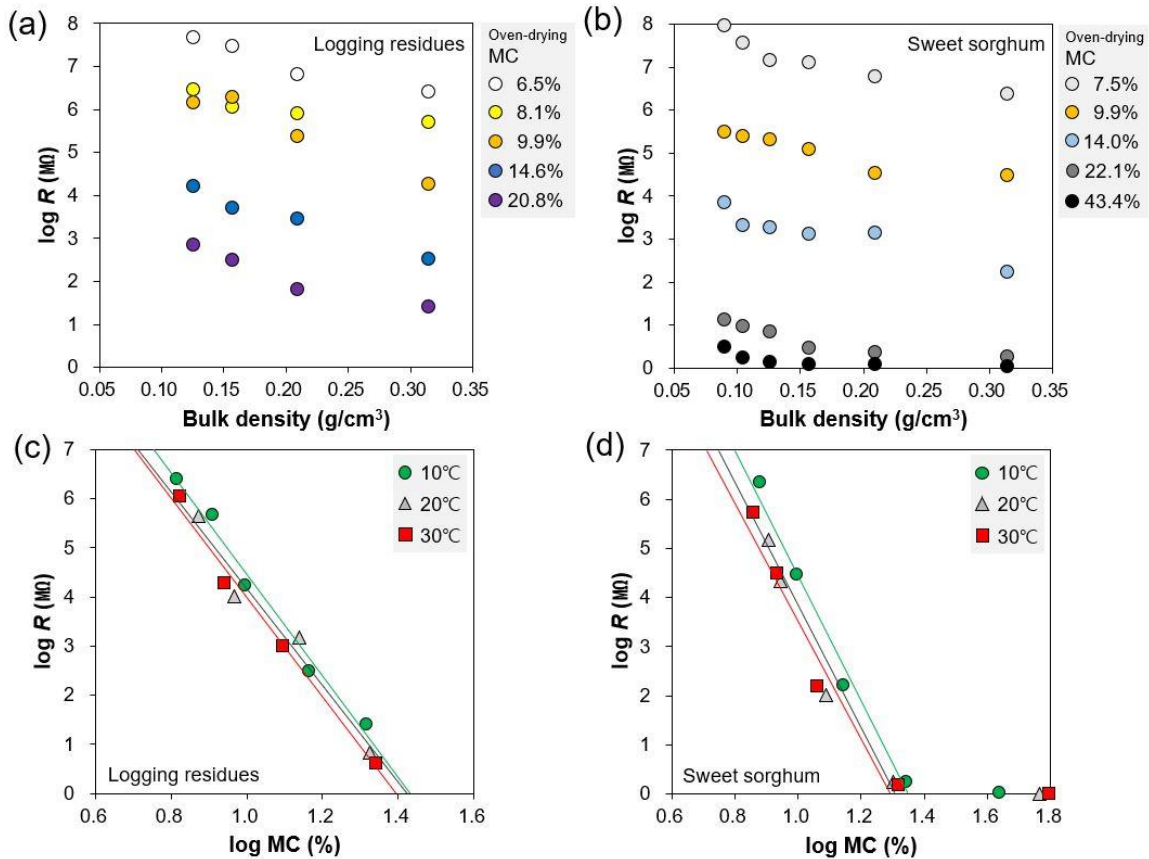


Fig. 6. Changes in electrical resistance with increasing bulk densities of logging residues (a) and sweet sorghum (b) at a temperature of 10°C, and relationship between moisture content and electrical resistance of logging residues (c) and sweet sorghum (d). Note: *R*, resistance to electricity

Table 4. Simple Linear Regression Equations between Electrical Resistance and Moisture Content below the Fiber Saturation Point

Biomass	Temperature	Regression Equation	R ²
Logging residue	10°C	$\log R$ (M Ω) = 14.765 – 10.316 $\log M$	0.984
	20°C	$\log R$ (M Ω) = 9.843 – 14.009 $\log M$	0.962
	30°C	$\log R$ (M Ω) = 10.104 – 14.098 $\log M$	0.989
Sweet sorghum	10°C	$\log R$ (M Ω) = 17.611 – 13.106 $\log M$	0.986
	20°C	$\log R$ (M Ω) = 15.944 – 12.253 $\log M$	0.965
	30°C	$\log R$ (M Ω) = 15.613 – 11.967 $\log M$	0.956

Notes: *R*, electrical resistance; *M*, moisture content (%); R², coefficient of determination

On a logarithmic scale, the relationship between the electrical resistance and MC was linear, with high coefficients of determination (Figs. 6c and 6d, Table 4). However, the linear relationship was valid only below the FSP. For sweet sorghum, MC was higher than FSP due to excessive moisture absorption at 95% RH. Therefore, a linear relationship could not be established, suggesting that separate models below and above the FSP are required for sophisticated moisture determination based on the electrical resistance.

Table 5 shows the prediction results of the ordinary least square regression models for the relationship among electrical resistance, MC, and temperature. The model prediction for logging residue achieved high performance, with an R^2 of 0.933 and RMSE of 0.505, whereas that for sweet sorghum was inferior, with an R^2 of 0.483 and RMSE of 1.657. However, in the limited MC range below the FSP, the model produced significantly improved performance, with R^2 and RMSE values of 0.833 and 0.891, respectively, suggesting that controlling the material's bulk density and MC range is essential for precisely determining the MC of biomass materials using electrical resistance-based methods.

Table 5. Ordinary Least Squares Regression Models Prediction Results for Moisture Content Determination of Biomass

Biomass	MC Range (%)	Regression Equation	Calibration		Prediction	
			R^2	RMSE	R^2	RMSE
Logging residue	5.4 to 22.0	$\log R (\text{M}\Omega) = 8.202 - 0.334 M - 0.012 T$	0.941	0.460	0.933	0.505
Sweet sorghum	7.2 to 62.5	$\log R (\text{M}\Omega) = 4.340 - 0.092 M + 0.005 T$	0.522	1.578	0.483	1.657
	7.2 to 22.1	$\log R (\text{M}\Omega) = 8.737 - 0.390 M - 0.035 T$	0.902	0.669	0.833	0.891

Notes: R , electrical resistance; M , moisture content (%); T , temperature ($^{\circ}\text{C}$); R^2 , coefficient of determination; RMSE, root mean square error

Multivariate Analysis

NIR spectral characteristics

Figures 7a and 7b show the second-derivative NIR spectra of logging residues and sweet sorghum straw in the 1300 to 2300 nm region. The 1437 and 1927 nm bands, with the two most prominent peaks in both materials, were assigned to water. The high humidification RH shifted the water peaks to the low-wavelength regions. The band shift is attributable to changes in the mobility and binding force of water molecules due to changes in the water content (Padalkar *et al.* 2013).

The spectral band at 1437 nm is rarely used for qualitative analysis but it may be helpful for quantitative purposes (Schwanninger *et al.* 2011). The increase in bulk density decreased the Euclidean distance between the spectra measured in triplicate (Figs. 7c and 7d). Hence, measuring the NIR spectra at bulk densities of 0.21 g/cm^3 or higher is desirable for both materials to obtain consistent NIR data.

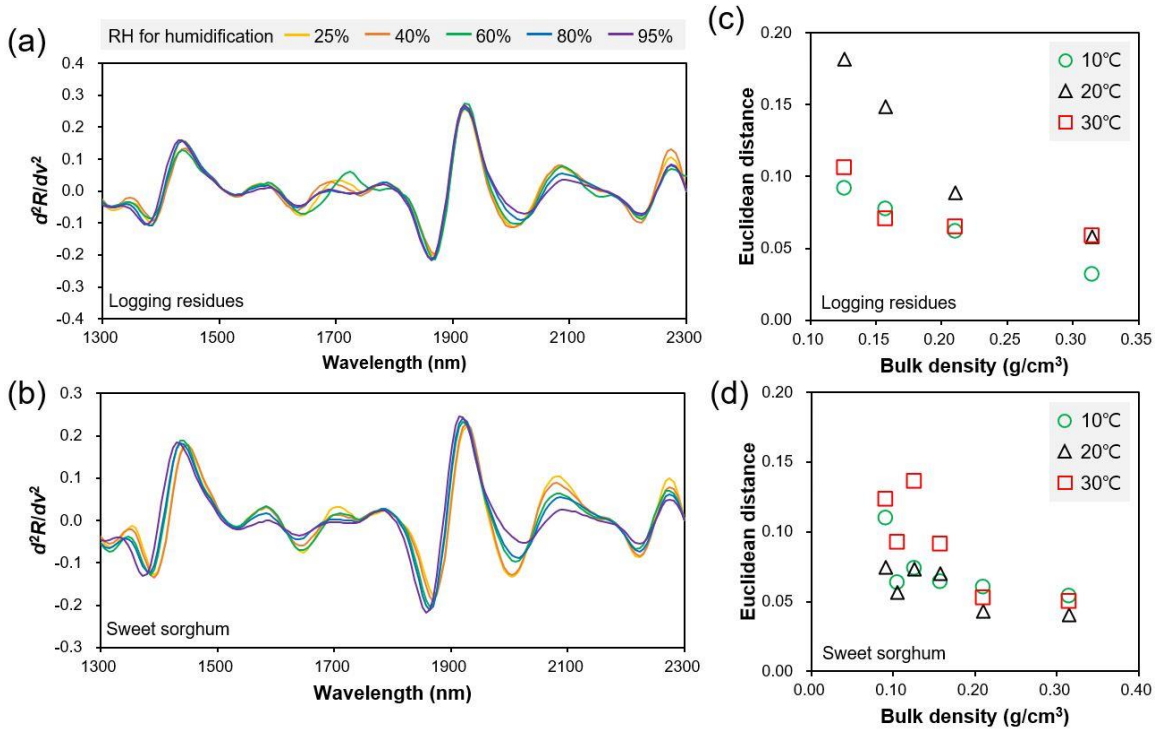


Fig. 7. Second-derivative near-infrared spectra of logging residue (a) and sorghum (b) samples compressed to a bulk density of 0.32 g/cm^3 at 20 °C, and Euclidean distances between spectra measured in triplicate at each density of logging residues (c) and sweet sorghum (d)

PCA and outliers

The clustering results of DBSCAN on the second-derivative NIR spectra of biomass materials were projected onto PC score plots (Fig. 8).

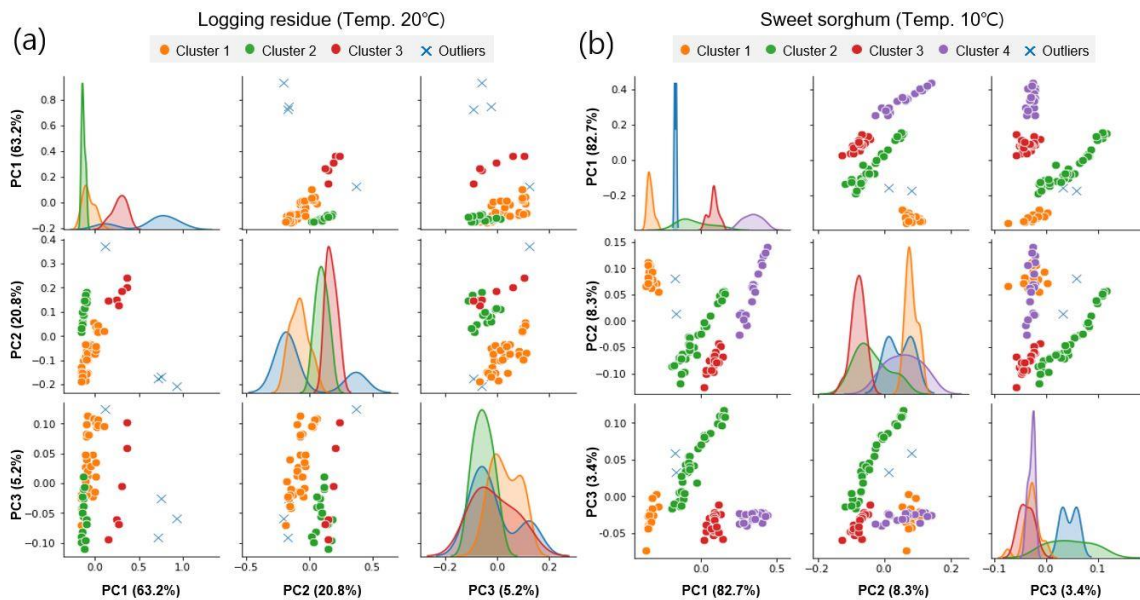


Fig. 8. Pair plots of principal component (PC) scores projected clustering by DBSCAN on near-infrared data with outliers of logging residues (a) and sweet sorghum (b). The percentage values in parentheses of the axis titles are the explained variance of the PC

DBSCAN identified four data points from the NIR spectra of logging residues measured at 20 °C and two from sweet sorghum at 10 °C as outliers. The generation of outliers was attributed to poor scans due to incomplete contact between the NIR probe and the sample at low bulk densities. In the score plots, the outliers did not belong to a cluster and were spatially located far from the other clusters. Although not exactly consistent with the predefined RH conditions, the clusters were formed based on the moisture level. The effectiveness of DBSCAN for outlier detection on NIR data was verified by comparing the performance of models built with datasets with and without outliers for MC prediction. The comparison is discussed in the subsection on the prediction model.

Figure 9 shows the score plots for the two PCs and the loadings of the first PCs of the logging residue and sweet sorghum. In the score plots, data points were arranged for each RH condition along PC1 for both materials; the higher the MC, the higher the PC1 score. In the sweet sorghum score, the data points were grouped by temperature under humidification with a specific RH. The loading plots for the first PCs of logging residue and sweet sorghum suggest that the 1437 and 1927 nm bands reveal the moisture level of the materials. The band at 2087 nm, representing the O–H stretching vibration of cellulose and hemicellulose (Schimleck *et al.* 1997), also had a moderate contribution.

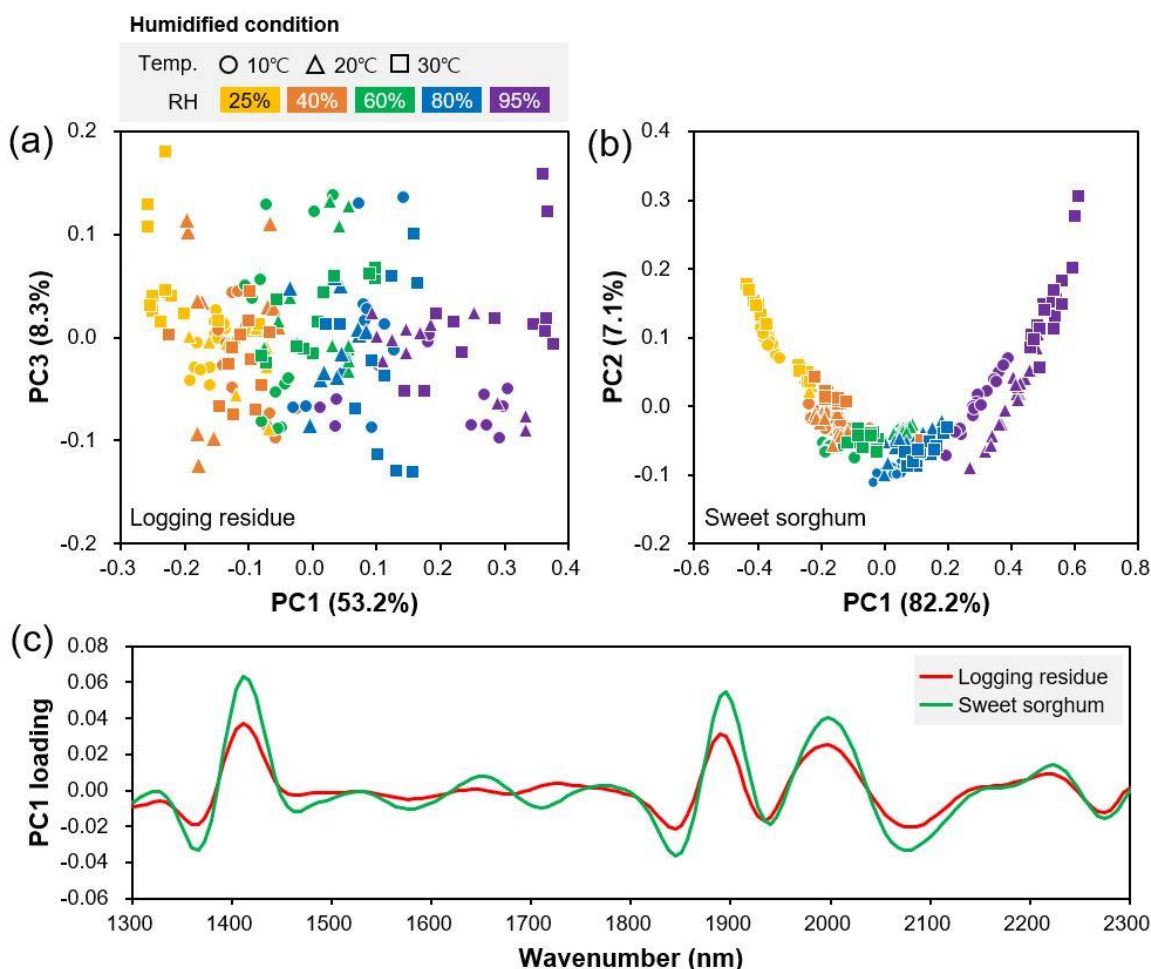


Fig. 9. Principal component analysis (PCA) score plots on two PCs in second-derivative NIR spectra of logging residues (a) and sweet sorghum (b) and loadings of the first PC for both materials. Percentages in parentheses (a and b) are scores of explained variance for each PC

Prediction models for NIR data

PLSR models built with the NIR spectra of logging residues and sweet sorghum were built for MC prediction. The scatter plots of the MC measured by the oven-drying method and the MC predicted by the PLSR model are presented in Fig. 10. Outliers in the dataset significantly deteriorated the prediction ability of the model. In the MC prediction of a model built with NIR data with outliers, several data points (*i.e.*, outliers) were far from the calibration line (Fig. 10a). In contrast, the prediction of a model built with data without outliers was similar to that of the calibration, with high R^2 and low RMSE values (Fig. 10b). These results imply the need for data preprocessing, such as outlier removal in building predictive models using NIR data and indicate that DBSCAN is an effective technique for detecting outliers in the NIR spectra.

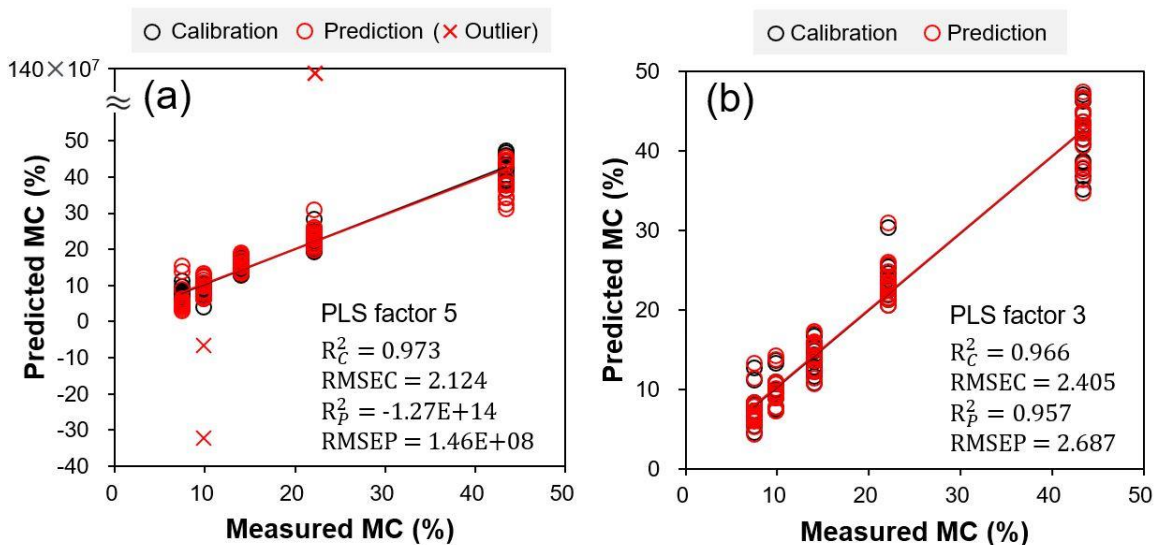


Fig. 10. Scatter plots of prediction results at a temperature of 10°C for moisture prediction models built with near-infrared data with outliers (a) and without outliers (b) in sweet sorghum. Notes: R_C^2 , coefficient of determination for calibration; RMSEC, root mean square error of calibration; R_P^2 , coefficient of determination for prediction; RMSEP, root mean square error for prediction

Spectral data processing using the second-derivative transform improved the predictions of the PLSR models. In all cases tested, models built with the second-derivative NIR spectra achieved higher R^2 and lower RMSE values with equal or lower PLS factors than those built with the original NIR spectra (Table 6). The best MC prediction performance was achieved by models built with the second derivative NIR spectra measured at 30 °C for both materials, with R^2 and RMSE for logging residue of 0.973 and 0.981, respectively, and 0.978 and 3.048 for sweet sorghum, respectively.

The models built using the total NIR data measured at all temperatures also showed good prediction performance for both materials. The model built with the total NIR data of logging residue achieved an R^2 of 0.942 and RMSE of 1.328, which were better than those for the model built with data measured at 10 and 20°C. The R^2 and RMSE values of the model built with the total data of sweet sorghum were 0.958 and 3.681, respectively. These results suggest that PLSR models can predict the MC of biomass materials with high precision within a temperature range of 10 to 30 °C, regardless of the band shift caused by

temperature fluctuations (Thygesen and Lundqvist 2000). The construction of PLSR models with NIR spectra is a promising approach for determining the MCs of logging residue and sweet sorghum, irrespective of the change in moisture state within the temperature fluctuations tested. In addition, the models were established through k-fold cross-validation with datasets separated by the bulk density of the materials. This means that MC prediction is possible regardless of the bulk density of materials, in contrast to electrical resistance-based models. The NIR-based method that does not require material compaction is likely more promising for industrial applications as it allows online or inline measurements without disrupting the process flow. Because the prediction models determine local MCs, multi-point measurements are desirable for a more reliable evaluation. Additionally, the model predictions are valid within the MC range tested in this study. Hence, data and model updates should be preceded to determine the MC outside the range.

Table 6. Performance of PLS Regression Models Built with Near-Infrared Spectra for Predicting Moisture Content of Biomass

Biomass	Data	NIR Spectrum	PLS Factor	Calibration		Prediction	
				R ²	RMSE	R ²	RMSE
Logging residue	Total	Original	8	0.905	1.709	0.875	1.958
		2nd derivative	7	0.959	1.124	0.942	1.328
	10 °C	Original	4	0.917	1.469	0.886	1.725
		2nd derivative	4	0.956	1.072	0.923	1.419
	20 °C	Original	4	0.873	1.923	0.808	2.364
		2nd derivative	3	0.946	1.252	0.929	1.436
	30 °C	Original	6	0.951	1.321	0.927	1.618
		2nd derivative	4	0.984	0.746	0.973	0.981
Sweet sorghum	Total	Original	6	0.955	3.786	0.948	4.094
		2nd derivative	6	0.968	3.177	0.958	3.681
	10 °C	Original	5	0.972	2.161	0.924	3.578
		2nd derivative	3	0.966	2.405	0.957	3.687
	20 °C	Original	7	0.981	2.572	0.969	3.331
		2nd derivative	4	0.985	2.290	0.972	3.182
	30 °C	Original	6	0.979	2.981	0.970	3.569
		2nd derivative	6	0.986	2.441	0.978	3.048

Note: PLS, partial least squares; R², coefficient of determination; RMSE, root mean square error

CONCLUSIONS

1. As the loose agglomeration of biomass fragments impedes the continuity of the charge transfer path, it was desirable to increase bulk density through material compression for precise moisture determination when using the electrical resistance method.
2. The calculated correction factor reduced the root-mean-squared error (RMSE) of the commercial moisture meter for logging residues and sweet sorghum. The electrical resistance-based ordinary least squares regression (OLSR) models achieved better predictions for logging residues than sweet sorghum, and the performance of the models for both materials was valid below the fiber saturation point (FSP).

3. The near infrared (NIR) spectra were stabilized at relatively sparse agglomeration of sample fragments, and the NIR-based models could predict the moisture content (MC) regardless of the bulk density of the materials.
4. Data preprocessing by second derivative transformation and outlier removal on the NIR data improved the prediction performance of the models.

ACKNOWLEDGEMENTS

This research was supported by the Nano Material Technology Development Program through the National Research Foundation of Korea (NRF) funded by the Ministry of Science and ICT (grant number:2021M3H4A3A02086904). We would like to thank Editage (www.editage.co.kr) for English language editing.

REFERENCES CITED

- Abdi, H. (2010). "Partial least squares regression and projection on latent structure regression (PLS regression)," *Wiley Interdisciplinary Reviews: Computational Statistics* 2(1), 97-106. DOI: 10.1002/wics.51
- Ashman, J. M., Jones, J. M., and Williams, A. (2018). "Some characteristics of the self-heating of the large scale storage of biomass," *Fuel Processing Technology* 174, 1-8. DOI: 10.1016/j.fuproc.2018.02.004
- Bergman, R. (2010). "Drying and control of moisture content and dimensional changes," in: *Wood Handbook: Wood as an Engineering Material*, Forest Products Laboratory, Forest Service, United States Department of Agriculture, Madison, WI, USA.
- Björngrim, N., Hagman, O., and Wang, X. A. (2016). "Moisture content monitoring of a timber footbridge," *BioResources* 11(2), 3904-3913. DOI: 10.15376/biores.11.2.3904-3913
- Bouckaert, S., Pales, A. F., McGlade, C., Remme, U., Wanner, B., Varro, L., D'Ambrosio, D., and Spencer, T. (2021). *Net Zero by 2050: A Road Map for the Global Energy Sector*, International Energy Agency, Paris, France.
- Brischke, C., Rapp, A. O., and Bayerbach, R. (2008). "Measurement system for long-term recording of wood moisture content with internal conductively glued electrodes," *Building and Environment* 43(10), 1566-1574. DOI: 10.1016/j.buildenv.2007.10.002
- Cardoso, C. R., Oliveira, T. J. P., Santana Junior, J. A., and Ataíde, C. H. (2013). "Physical characterization of sweet sorghum bagasse, tobacco residue, soy hull and fiber sorghum bagasse particles: Density, particle size and shape distributions," *Powder Technology* 245, 105-114. DOI: 10.1016/j.powtec.2013.04.029
- Chang, Y. S., Yang, S. Y., Chung, H., Kang, K. Y., Choi, J. W., Choi, I. G., and Yeo, H. (2015). "Development of moisture content prediction model for *Larix kaempferi* sawdust using near infrared spectroscopy," *Journal of the Korean Wood Science and Technology* 43(3), 304-310. DOI: 10.5658/WOOD.2015.43.3.304
- Costa, J. A. V., and De Morais, M. G. (2011). "The role of biochemical engineering in the production of biofuels from microalgae," *Bioresource Technology* 102(1), 2-9.

DOI: 10.1016/j.biortech.2010.06.014

- Cywar, R. M., Rorrer, N. A., Hoyt, C. B., Beckham, G. T., and Chen, E. Y. -X. (2022). “Bio-based polymers with performance-advantaged properties,” *Nature Reviews Materials* 7(2), 83-103. DOI: 10.1038/s41578-021-00363-3
- Dietsch, P., Franke, S., Franke, B., Gamper, A., and Winter, S. (2015). “Methods to determine wood moisture content and their applicability in monitoring concepts,” *Journal of Civil Structural Health Monitoring* 5(2), 115-127. DOI: 10.1007/s13349-014-0082-7
- Ekefre, D. E., Mahapatra, A. K., Latimore Jr, M., Bellmer, D. D., Jena, U., Whitehead, G. J., and Williams, A. L. (2017). “Evaluation of three cultivars of sweet sorghum as feedstocks for ethanol production in the Southeast United States,” *Heliyon* 3(12), article e00490. DOI: 10.1016/j.heliyon.2017.e00490
- Eliasson, L., Anerud, E., Grönlund, Ö., and von Hofsten, H. (2020). “Managing moisture content during storage of logging residues at landings – Effects of coverage strategies,” *Renewable Energy* 145, 2510-2515. DOI: 10.1016/j.renene.2019.07.159
- Eom, C. D., Han, Y. J., Chang, Y. S., Park, J. H., Choi, J. W., Choi, I. G., and Yeo, H. (2010). “Evaluation of surface moisture content of *Liriodendron tulipifera* wood in the hygroscopic range using NIR spectroscopy,” *Journal of the Korean Wood Science and Technology* 38(6), 526-531. DOI: 10.5658/WOOD.2010.38.6.526
- Erickson, B., Nelson, P., and Winters, P. (2012). “Perspective on opportunities in industrial biotechnology in renewable chemicals,” *Biotechnology Journal* 7(2), 176-185. DOI: 10.1002/biot.201100069
- Ester, M., Kriegel, H. P., Sander, J., and Xu, X. (1996). “A density-based algorithm for discovering clusters in large spatial databases with noise,” in: *Proceedings of the Second International Conference on Knowledge Discovery and Data Mining*, Portland, OR, USA, 2–4 August 1996.
- Fajardo, A. R., Pereira, A. G. B., and Muniz, E. C. (2015). “Hydrogels nanocomposites based on crystals, whiskers and fibrils derived from biopolymers,” in: *Eco-Friendly Polymer Nanocomposites*. Springer, New Delhi, India. DOI: 10.1007/978-81-322-2473-0_2
- Filbakk, T., Høibø, O., and Nurmi, J. (2011). “Modelling natural drying efficiency in covered and uncovered piles of whole broadleaf trees for energy use,” *Biomass and Bioenergy* 35(1), 454-463. DOI: 10.1016/j.biombioe.2010.09.003
- Gejdoš, M., and Lieskovský, M. (2021). “Wood chip storage in small scale piles as a tool to eliminate selected risks,” *Forests* 12(3), article 289. DOI: 10.3390/f12030289
- Gillis, C. M., Stephens, W. C., and Peralta, P. N. (2001). “Moisture meter correction factors for four Brazilian wood species,” *Forest Products Journal* 51(4), 83-86.
- Govett, R., Mace, T., and Bowe, S. (2010). “A practical guide for the determination of moisture content of woody biomass,” *International Tropical Timber Organization*, (<http://www.tropicaltimber.info/wp-content/uploads/2015/06/A-Practical-Guide-for-Determination-of-Moisture-Content-of-Woody-Biomass-2010GovettR.University-of-WisconsinStevens-Point20-pp.pdf>.) Accessed 11 Jan 2023.
- Horikawa, Y. (2017). “Assessment of cellulose structural variety from different origins using near infrared spectroscopy,” *Cellulose* 24(12), 5313-5325. DOI: 10.1007/s10570-017-1518-0
- Hwang, S. W, Horikawa, Y., Lee, W. H., Sugiyama, J. (2016). “Identification of *Pinus* species related to historic architecture in Korea using NIR chemometric approaches,”

- Journal Wood Science* 62(2), 156-167. DOI: 10.1007/s10086-016-1540-0
- Hwang, S. W., Hwang, S. Y., Lee, T., Ahn, K. S., Pang, S. J., Park, J., Oh, J. K., Kwak, H. W., and Yeo, H. (2021a). "Investigation of electrical characteristics using various electrodes for evaluating the moisture content in wood," *BioResources* 16(4), 7040-7055. DOI: 10.15376/biores.16.4.7040-7055
- Hwang, S. W., Hwang, U. T., Jo, K., Lee, T., Park, J., Kim, J. C., Kwak, H. W., Choi, I. G., and Yeo, H. (2021b). "NIR-chemometric approaches for evaluating carbonization characteristics of hydrothermally carbonized lignin. *Scientific Reports* 11(1), article 16979. DOI: 10.1038/s41598-021-96461-x
- Hwang, U. T., Bae, J., Lee, T., Hwang, S. Y., Kim, J. C., Park, J., Choi, I. G., Kwak, H. W., Hwang, S. W., and Yeo, H. (2021c). "Analysis of carbonization behavior of hydrochar produced by hydrothermal carbonization of lignin and development of a prediction model for carbonization degree using near-infrared spectroscopy," *Journal of the Korean Wood Science and Technology* 49(3), 213-225. DOI: 10.5658/WOOD.2021.49.3.213
- Hwang, S. W., Chung, H., Lee, T., Ahn, K. S., Pang, S. J., Kim, J. Y., Bang, J., Jung, M., Oh, J. K., Kwak, H. W., and Yeo, H. (2023). "Dimensional behavior of nail-laminated timber-concrete composite caused by changes in ambient air, and correlation among temperature, relative humidity, and strain," *BioResources* 18(1), 1637-1652. DOI: 10.15376/biores.18.1.1637-1652
- Inagaki, T., Siesler, H. W., Mitsui, K., and Tsuchikawa, S. (2010). "Difference of the crystal structure of cellulose in wood after hydrothermal and aging degradation: A NIR spectroscopy and XRD study," *Biomacromolecules* 11(9), 2300-2305. DOI: 10.1021/bm100403y
- Jensen, P. D., Hartmann, H., Böhm, T., Temmerman, M., Rabier, F., and Morsing, M. (2006). "Moisture content determination in solid biofuels by dielectric and NIR reflection methods," *Biomass and Bioenergy* 30(11), 935-943. DOI: 10.1016/j.biombioe.2006.06.005
- Julrat, S., and Trabelsi, S. (2019). "In-line microwave reflection measurement technique for determining moisture content of biomass material," *Biosystems Engineering* 188, 24-30. DOI: 10.1016/j.biosystemseng.2019.09.013
- Kalyani, P., and Anitha, A. (2013). "Biomass carbon & its prospects in electrochemical energy systems," *International Journal of Hydrogen Energy* 38(10), 4034-4045. DOI: 10.1016/j.ijhydene.2013.01.048
- Krzyżaniak, M., Stolarski, M. J., Niksa, D., Tworkowski, J., and Szczukowski, S. (2016). "Effect of storage methods on willow chips quality," *Biomass and Bioenergy* 92, 61-69. DOI: 10.1016/j.biombioe.2016.06.007
- Lahtela, V., Hämäläinen, K., and Kärki, T. (2014). "The effects of preservatives on the properties of wood after modification – A review," *Baltic forestry* 20(1), 189-203.
- Langholtz, M. H., Stokes, B. J., and Eaton, L. M. (2016). *2016 Billion-Ton Report: Advancing Domestic Resources for a Thriving Bioeconomy, Volume 1 Economic Availability of Feedstock*, Oak Ridge National Laboratory, Oak Ridge, TN, USA. DOI: 10.2172/1271651
- McKendry, P. (2002). "Energy production from biomass (part 1): Overview of biomass," *Bioresource Technology* 83(1), 37-46. DOI: 10.1016/S0960-8524(01)00118-3

- Mitsui, K., Inagaki, T., and Tsuchikawa, S. (2008). "Monitoring of hydroxyl groups in wood during heat treatment using NIR spectroscopy," *Biomacromolecules* 9(1), 286-288. DOI: 10.1021/bm7008069
- Molino, A., Chianese, S., and Musmarra, D. (2016). "Biomass gasification technology: The state of the art overview," *Journal of Energy Chemistry* 25(1), 10-25. DOI: 10.1016/j.jechem.2015.11.005
- Padalkar, M. V., Spencer, R. G., and Pleshko, N. (2013). "Near infrared spectroscopic evaluation of water in hyaline cartilage," *Annals of Biomedical Engineering* 41(11), 2426-2436. DOI: 10.1007/s10439-013-0844-0
- Park, S. A., Jeon, H., Kim, H., Shin, S. H., Choy, S., Hwang, D. S., Koo, J. M., Jegal, J., Hwang, S. Y., Park, J., and Oh, D. X. (2019). "Sustainable and recyclable super engineering thermoplastic from biorenewable monomer," *Nature Communications* 10(1), article 2601. DOI: 10.1038/s41467-019-10582-6
- Qian, E. W. (2014) "Pretreatment and saccharification of lignocellulosic biomass," in: *Research Approaches to Sustainable Biomass Systems*, Academic Press, Cambridge, MA, USA.
- Samuelsson, R., Burvall, J., and Jirjis, R. (2006). "Comparison of different methods for the determination of moisture content in biomass," *Biomass and Bioenergy* 30(11), 929-934. DOI: 10.1016/j.biombioe.2006.06.004
- Savitzky, A., and Golay, M. J. E. (1964). "Smoothing and differentiation of data by simplified least squares procedures," *Analytical Chemistry* 36(8), 1627-1639. DOI: 10.1021/ac60214a047
- Schimleck, L. R., Wright, P. J., Michell, A. J., and Wallis, A. A. (1997). "Near-infrared spectra and chemical compositions of *E. globulus* and *E. nitens* plantation woods," *Appita Journal* 50(1), 40-46.
- Schwanninger, M., Rodrigues, J. C., and Fackler, K. (2011). "A review of band assignments in near infrared spectra of wood and wood components," *Journal of Near Infrared Spectroscopy* 19(5), 287-308. DOI: 10.1255/jnirs.955
- Suchomel, J., Belanová, K., Gejdoš, M., Němec, M., Danihelová, A., and Mašková, Z. (2014). "Analysis of fungi in wood chip storage piles," *BioResources* 9(3), 4410-4420. DOI: 10.15376/biores.9.3.4410-4420
- Swinton, S. M., Dulys, F., and Klammer, S. S. H. (2021). "Why biomass residue is not as plentiful as it looks: case study on economic supply of logging residues," *Applied Economic Perspectives and Policy* 43(3), 1003-1025. DOI: 10.1002/aapp.13067
- Takagaki, A., Nishimura, S., and Ebitani, K. (2012). "Catalytic transformations of biomass-derived materials into value-added chemicals," *Catalysis Surveys from Asia* 16(3), 164-182. DOI: 10.1007/s10563-012-9142-3
- Tang, J. P., Lam, H. L., Aziz, M. K. A., and Morad, N. A. (2014). "Biomass characteristics index: A numerical approach in palm bio-energy estimation," *Computer Aided Chemical Engineering* 33, 1093-1098. DOI: 10.1016/B978-0-444-63455-9.50017-9
- Thygesen, L. G., and Lundqvist, S. O. (2000). "NIR measurement of moisture content in wood under unstable temperature conditions. Part 1. Thermal effects in near infrared spectra of wood," *Journal of Near Infrared Spectroscopy* 8(3), 183-189. DOI: 10.1255/jnirs.277
- United Nations. (2020). *2050 Carbon Neutral Strategy of the Republic of Korea*. <https://unfccc.int/documents/267683>. Accessed 18 Aug 2022

- Via, B. K., Zhou, C., Acquah, G., Jiang, W., and Eckhardt, L. (2014). “Near infrared spectroscopy calibration for wood chemistry: Which chemometric technique is best for prediction and interpretation?” *Sensors* 14(8), 13532-13547. DOI: 10.3390/s140813532
- Yang, S. Y., Han, Y., Park, J. H., Chung, H., Eom, C. D., and Yeo, H. (2015). “Moisture content prediction model development for major domestic wood species using near infrared spectroscopy,” *Journal of the Korean Wood Science and Technology* 43(3), 311-319. DOI: 10.5658/WOOD.2015.43.3.311
- Zhang, M. H., Luypaert, J., Fernández Pierna, J. A., Xu, Q. S., and Massart, D. L. (2004). “Determination of total antioxidant capacity in green tea by near-infrared spectroscopy and multivariate calibration,” *Talanta* 62(1), 25-35. DOI: 10.1016/S0039-9140(03)00397-7

Article submitted: December 8, 2022; Peer review completed: January 7, 2023; Revised version received and accepted: January 20, 2023; Published: January 30, 2023.
DOI: 10.15376/biores.18.1.2064-2082